Asian Journal of Chemistry; Vol. 32, No. 12 (2020), 3019-3023

ASIAN JOURNAL OF CHEMISTRY

https://doi.org/10.14233/ajchem.2020.22854

Effect of Sulfur Doped Nanotitania for Degradation of Remazol Yellow and Phenol

POSMAN MANURUNG[1,*], RUDY SITUMEANG[2], PERDINAN SINUHAJI[3] and SIMON SEMBIRING[1]

[1]Department of Physics, Faculty of Mathematics and Natural Sciences, University of Lampung, Bandar Lampung 35145, Indonesia
[2]Department of Chemistry, Faculty of Mathematics and Natural Sciences, University of Lampung, Lampung 35145, Indonesia
[3]Department of Physics, Faculty of Mathematics and Natural Sciences, University of North Sumatera, Sumatera Utara 20222, Indonesia

*Corresponding author: E-mail: reip65@yahoo.com

Received: 10 June 2020; *Accepted*: 28 August 2020; *Published online*: 7 December 2020; AJC-20133

Nanocrystalline TiO_2 and sulfur-doped TiO_2 were synthesized using the sol-gel method. Tween-80, titanium tetraisopropoxide (TTIP), and sulfuric acid were employed as raw materials for the synthesis of TiO_2. All the synthesized samples were heated for 3 h at 500 ºC. Each cell parameter of the prepared samples was explored by employing the Rietveld refinement of X-ray diffraction (XRD) patterns. For sulfur-doped TiO_2 and TiO_2 samples, considerable differences were observed in their cell parameters. Under ultraviolet (UV) irradiation, the phenol and remazol yellow (RY) photodegradation of the sintered samples was analyzed. Physical properties were studied using Brunauer-Emmett-Teller (BET) and transmission electron microscopy (TEM) analyzes to measure the surface area. The XRD results confirmed that except nano-anatase, no other phase was present in any sample. The particle size range is 10-15 nm. BET surface results showed that doping concentrations influenced the surface area. On the samples with a larger surface area, photodegradation is superior, which coincides with a higher doping concentration.

Keywords: Nanotitania, Remazol yellow, Phenol, Photodegradation, Tween-80.

INTRODUCTION

Nanotechnology is used for manipulating atoms, elements or molecules to acquire new properties [1]. For revolution in engineering and materials science, nanotechnology plays a crucial role for obtaining novel materials with excellent optical, electrical, mechanical and magnetic properties. The wide scopes of nanotechnology include the study of nano-physics, nano-chemistry, nanomaterial science, nanoelectronics, nanoscale, nanometrology and nanobionics [2-4].

Among various nanomaterials, the material nano-titania remains under development. Nanotitania is widely employed in numerous fields such as solar cells and water purification [5]. It is most widely used as photocatalysts [6] and antibacterial agent [7]. Titanium dioxide occurs in three polymorphic forms: rutile, brookite and anatase. The thermodynamic stability of rutile is higher than that of anatase and under pellet conditions, rutile structures are thermodynamically stable. However, thermodynamic experiments have shown that when the size of particles is in a nanometer range, anatase can exhibit higher stability than rutile. The anatase phase is metastable and can be transformed into the rutile phase with the heating treatment. The thermodynamic stability of rutile is higher at room pressure than that of anatase and brookite. However, thermodynamic stability is particle size dependent, which contribute to free surface energy.

Nanotitania is widely employed as photocatalysis material because it is stable, inexpensive and non-poison. Currently, nanotitania is used in water purification, air cleaning, self-cleaning, anti-tumor applications [8], whitening [9], dye-sensitized solar cells [10] and anti-blur applications [11]. Among three titania structures, for photocatalysis, anatase is a suitable candidate. The gap energy of the anatase phase of 3.2 eV [12] corresponds to the solar UV irradiation. To enhance the photocatalysis of nanotitania, its gap energy must be narrowed through doping addition. A few commonly doped materials to nanotitania include carbon [13], nitrogen [14], fluor [15] and sulfur [16].

In this study, nanotitania was doped with sulfur. Wang *et al.* [17] conducted a study by using sulfur as a dopant for

nanotitania. They used tetrabutyl titanate and alcohol as a precursor and solvent, respectively to synthesize nanotitania. In their study, 1.21% sulfur doping provided better photoabsorption properties than pure titania. Additionally, the average size of sulfur-doped nanotitania (9.73 nm) is smaller than that of pure nanotitania (17.36 nm). This result indicated that sulfur-doped nanotitania exhibited a better activity as a photo-catalyst in L-acid photodegradation than pure nanotitania did. Thus, in this study, the effect of sulfuric acid as a sulfur-dopant source for the fabrication of nano-titania by using titanium tetraisopropoxide (TTIP) as the base material on the photocatalysis activity of nanotitania was investigated.

In this work, the XRD results of the non-doped and sulfur-doped nanotitania at 500 ºC were investigated. The effects of non-doped and doped nanotitania on the degradation of phenol and remazol yellow was discussed by using BET, TEM and UV-Vis spectroscopic analyses.

EXPERIMENTAL

Titanium tetraisopropoxide (TTIP) was purchased from Aldrich, while sulfuric acid, isopropanol and surfactant Tween-80 were procured from Merck, USA. All materials were used without purification.

Powder XRD patterns were obtained on XPERT PRO PANalytical using CuKα radiation (λ = 1.54060 Å) produced at 40 kV and 30 mA. The patterns were collected over a range 10-100º with a step size of 0.026º. TEM with SAED of JEOL JEM-1400 version 1.0 was used to find microstructure together with measuring particle size. A Quantachrome TouchWin v1.2 was used to examine the BET surface area. UV lamp of 150 W from Osram was used to conduct the photocatalysis experiment. The lamp was set perpendicularly above sample at 30 cm. UV-visible spectrum was recorded with Cary 100 version 12.00.

Methodology: Sulfur-doped and non-doped nanotitania were synthesized using the sol-gel method. First, 10 g of Tween-80 was added to 80 mL of isopropanol in a 200 mL glass beaker and the mixture was stirred for 30 min at 200 rpm. After a homogeneous solution was obtained, titanium tetraisopropoxide (TTIP) was added dropwise and the solution was stirred for 1 h. Subsequently, the sulfur dopant was added to the solution and again stirred for 24 h. The solution was heated to 100 and then to 150 ºC for drying. Afterwards, a powder was placed in a crucible, which was then heated in a furnace at 500 ºC for 3 h. The dried powder was crushed using an agate mortar to acquire a nanotitania powder. Table-1 presents the samples with different amounts of sulfur doping.

TABLE-1
COMPOSITION OF UNDOPED AND SULFUR-DOPED NANO-TITANIA

Sample	Tween-80 (g)	Isopropanol (mL)	TTIP (mL)	H_2SO_4 (mL)
A	10	80	6.8	–
B	10	80	6.8	1.24
C	10	80	6.8	3.10
D	10	80	6.8	6.20
E	10	80	6.8	12.4

Photocatalysis: The photocatalytic activity of each sample for phenol and remazol yellow decolourization was evaluated at ambient temperature. Remazol yellow solution (300 mL of 10 ppm) was mixed with 0.25 g of sulfur-doped and non-doped nano-titania powders separately and stirred under UV conditions. Then, 10 mL of the solution was taken out after each 10 min to examine remazol yellow decolourization using UV-vis spectroscopy.

The same procedure was followed for 20 ppm phenol. For phenol degradation, the solution was removed from glass beaker at 20, 40, 70, 100 and 140 min. Degradation of phenol was assumed to be more difficult than remazol yellow.

RESULTS AND DISCUSSION

XRD studies: Fig. 1 presents the XRD patterns of sulfur-doped nano-TiO_2 (B, C, D and E) and the non-doped sample (A). All the peaks in diffractogram represent anatase phase without the presence of the rutile or brookite phases. This finding indicated that the incorporation of small concentrations of sulfur to nanotitania does not result in a new phase. The results of the qualitative analysis showed diffraction peaks to be in line with the JCPDS file No. 21-1272 for anatase [18].

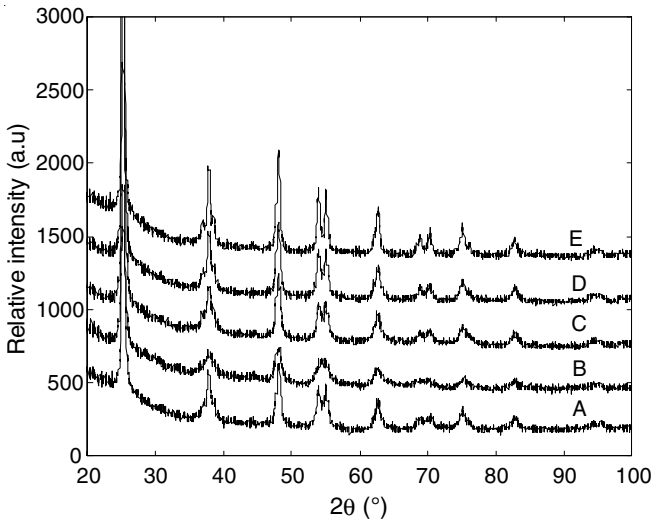

Fig. 1. Diffractogram of undoped (A) and doped nano TiO_2's (B,C,D and E). The wavelength of X-ray is 1.54056 Å

For all the samples, peak positions are the same. The strongest peak appeared at the position of 2θ of 25.34º (011), as reported in literature [19-21]. Among all the samples, only sample B exhibited a low intensity. If the diffractogram intensity is considered the crystalline level, sample B exhibits more amorphous phase than the other samples. According to the following Scherrer's equation, the average crystallite size for the non-doped and doped samples was 12 nm.

$$D = \frac{0.89\lambda}{\beta\cos\theta}$$

For the quantitative analysis of cell counting parameters, data were analysed by employing the Rietveld method. The model employed for anatase is reported earlier [22] and Rietica software was used in this study [23]. Before the quantitative

analysis, the input file was written in the program. After the program was run, the result was obtained as the output file. Fig. 2 presents a typical profile fit for XRD data of the non-doped sample A.

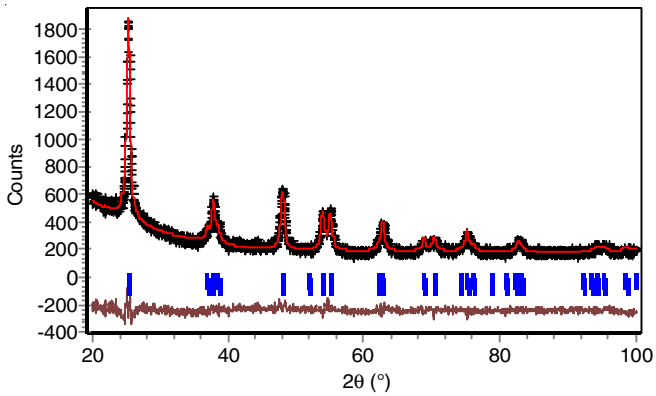

Fig. 2. XRD plot for sample A. Measured and calculated patterns are indicated by a cross and solid line respectively. Vertical bars represent the allowable peak positions for anatase. The wavelength of the X-ray is 1.54056 Å

By using the same model, Fig. 3 presents the optimal fit between the observed and calculated XRD patterns for the sulfur-doped sample E. The acceptable R_B fitting parameters and fit goodness of <2 and <1.6, respectively, indicate the good refinement quality of diffraction data. In addition to the density,

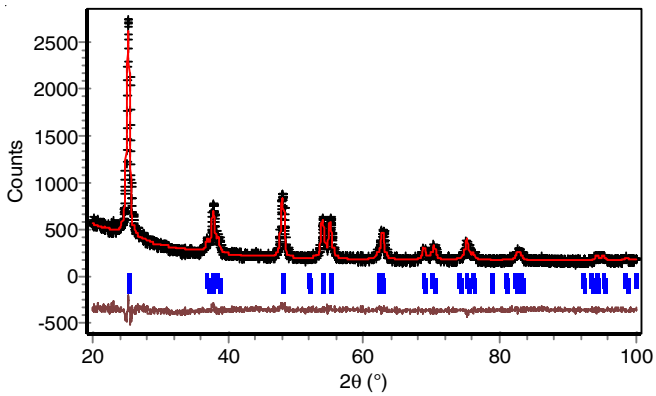

Fig. 3. XRD profile for sample E. Measured and calculated patterns are indicated by a cross and solid line respectively. Vertical bars represent the Bragg peak position for anatase

background, preferred orientation, atomic position, and peak shape, cell parameters can be recorded. Fig. 4 illustrates the cell parameters of all samples based on the Rietveld analysis.

The presence of sulfur doping did not change the cell parameter 'a', however, substantially changed the cell parameter 'c'. The presence of sulfur decreased the cell parameter 'c' and then, the parameter curve became relatively flat. The presence of dopant in bulk can decrease or increase the cell parameter. Janotti *et al*. [24] reported a sharp increase in the lattice parameter of $SrTiO_3$ after La doping. By contrast, the lattice parameter of CdO:Mn films decreased with an increase in Mn doping [25].

BET studies: The vacuum degassing of BET was obtained using SAA Qantachrome NOVA 1000e version 11.0. Nitrogen was the gas adsorbate used for measurement and bath temperature was maintained at 77.35 K. Fig. 5 illustrates the surface area of the sulfur-doped nano-titania and non-doped samples. The results of BET surface analyses revealed a considerable increase in the surface area resulting from the enhancement of the interfacial region caused by sulfur doping. For the highest doping in sample E, the maximum surface area was recorded. During the heating of samples, dislocations and point defects may have affected the increase in the surface area. In the samples, the higher was the sulfur doping, the larger was the number of defects, which increased the surface area. Paul and Mohanta [26] observed the same behaviour when they doped nano-TiO_2 with Eu through condensation. The high amounts of sulfur-doping considerably enhance the surface area. Sample E provided the highest BET value of 140 m^2/g,

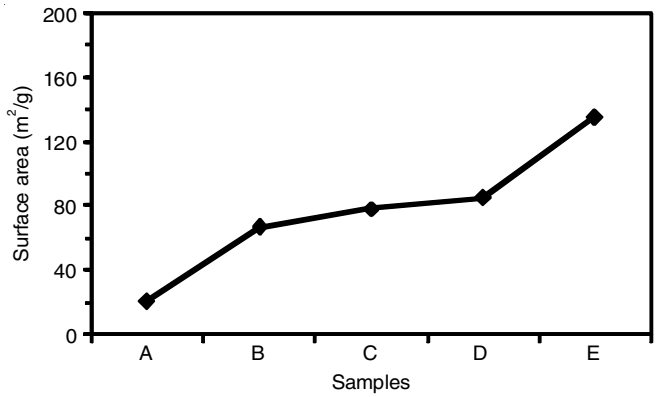

Fig. 5. Surface area of nano-titania and S-doped nanotitania

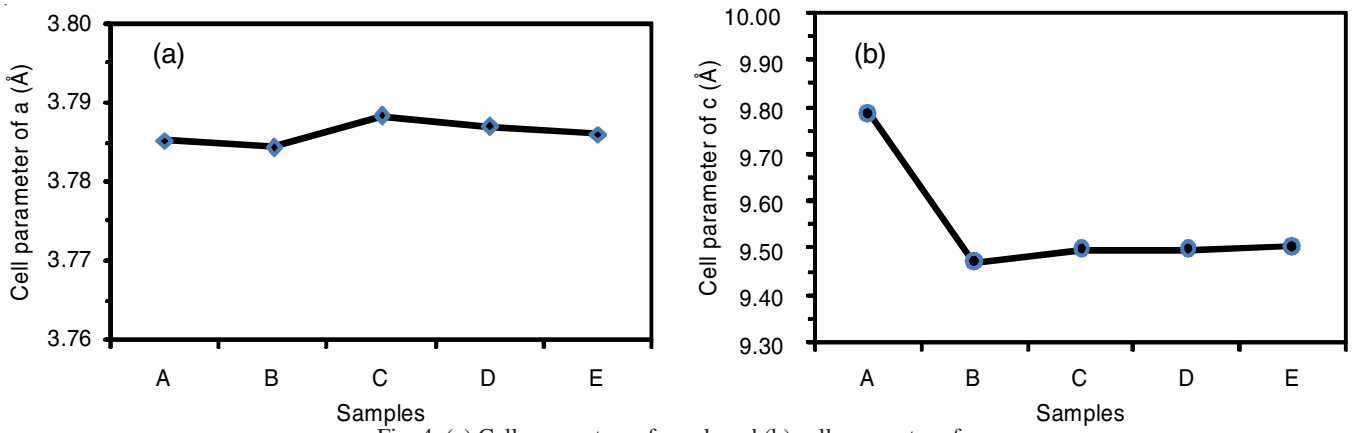

Fig. 4. (a) Cell parameters of a or b and (b) cell parameter of c

and the particle size of sample E was 12 nm, which indicated that higher sulfur doping can enhance the surface area of samples.

TEM studies: TEM was conducted for S-doped and pure TiO_2. Sample A was nano-titania without doping sulfur, *i.e.*, the sample was synthesized using Tween-80 and TTIP (Fig. 6a). All particles were trapped, which means that the particles were cohesive [27]. This phenomenon can be attributed to the surface area of sample A (Fig. 5), and the BET of sample A was only 30 m^2/g. The sulfur-doped samples (B, C, D and E) were not held together, which indicated that no cohesive behaviour was involved. According to imageJ software, size of the non-doped particles was in an order of 13 nm, which was considerably close to the particle size measured using Scherrer′s equation from the XRD data. Sample C exhibited the smallest size of 7 nm, which was lower than the value obtained using Scherrer′s equation. This value can be the optimum addition of sulfur for reducing the nanotitania particle size.

Photocatalysis studies: Remazol yellow is an artificial dye used in textile industries because it can easily be diluted in water. Because of its high decomposition temperature, pH and microbe resistance, remazol yellow present in sewage can potentially affect the environment, if not processed [28].

The photocatalytic activity of the samples was explored through remazol yellow and phenol degradation under UV irradiation as a model reaction. According to the remazol yellow spectra, dye degradation attained the peak position at the maximum wavelength of 411 nm (Fig. 7). The non-doped nano-titania sample (sample A) indicated that remazol yellow degradation was extremely slow even for the irradiation time of 50 min (Fig. 7), which implied that the capacity of non-doped nanotitania to degrade remazol yellow dye is considerably low. The same phenomenon was observed for sample B, which was doped with small amounts of sulfur. The photocatalytic activity of titania highly depends on the specific surface area and crystalline structure [29]. Remazol yellow degradation increased with an increase in the amounts of sulfur doping. Maximum degradation was achieved using sample E, which exhibited the highest BET.

In case of phenol, the peak position of phenol degradation was achieved at the maximum wavelength of 270 nm (Fig. 8). Phenol degradation was relatively more difficult than the degradation of other dyes. After 140 min, phenol degradation considerably decreased. The difficulties observed in phenol degradation were caused by its ring structure. Guo *et al*. [30] observed that during degradation, -OH radicals attack the aromatic phenol ring, which results in resorcinol, catechol, and hydroquinone formation. When an aromatic ring broke, first, malonic acid was formed, and then, short chain was formed to produce oxalic acid, maleic acid, formic acid and acetic acid. Finally, CO_2 was produced. From these degradation steps, irradiation required considerable time for degrading phenol and phenol derivative. This finding is supported by Sobcynski *et al*. [31], who reported 25% phenol degradation after 3 h of irradiation. Grabowska *et al*. [32] reported the mechanism for phenol degradation through TiO_2 [32], which required more time than the degradation of other dyes did.

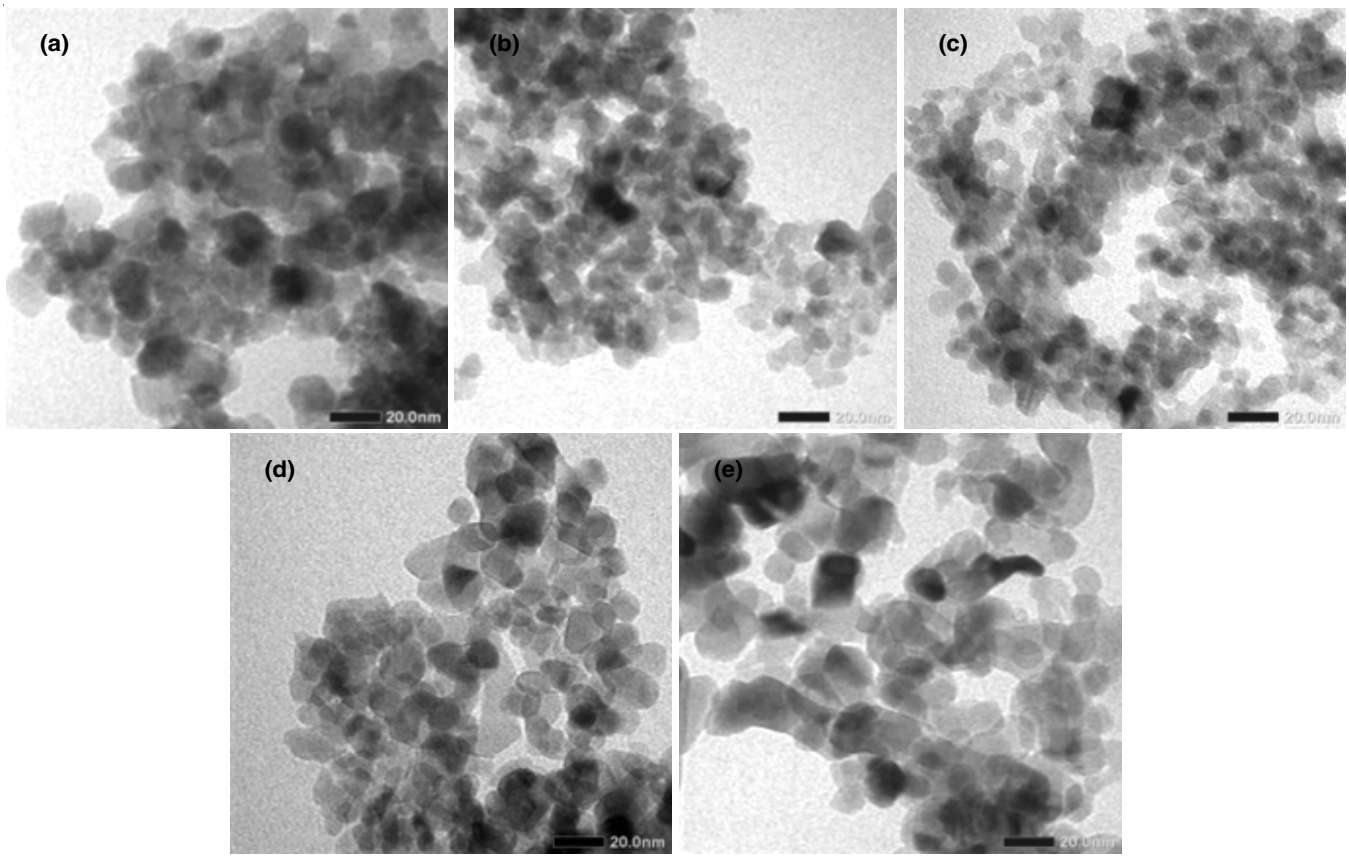

Fig. 6. TEM images of sample A, B, C, D and E. Bar scale = 20 nm

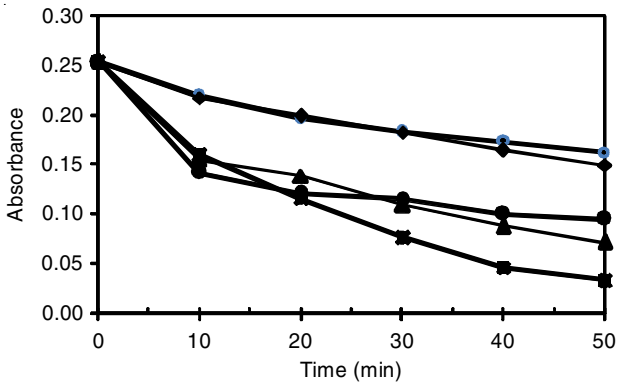

Fig. 7. Degradation of remazol yellow under UV ray for sample A, B, C, D and E (top-bottom) at peak position of λ = 411 nm

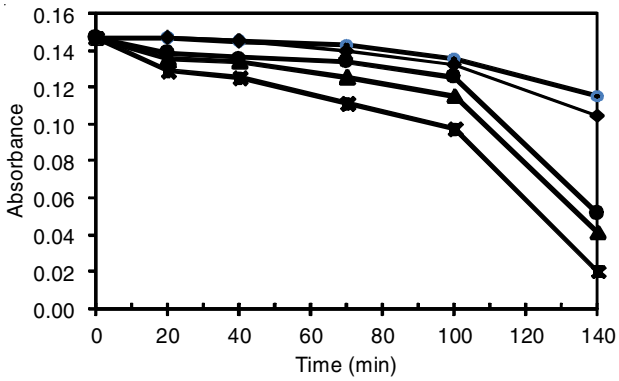

Fig. 8. Degradation of phenol (20 ppm) under UV ray for sample B, C, D and E (top-bottom) at the peak position of λ = 270 nm

Conclusion

In this work, the influence of sulfur doping in nano-titania for grain shape, crystal structure surface area and photocatalysis behaviour on phenol and remazol yellow dye was studied. The XRD data indicated that all the samples exhibited the anatase phase. The presence of sulfur doping considerably reduced the *c*-axis cell parameter. With an increase in sulfur doping, the surface area increased. Dislocations and point defects may have affected sulfur doping. The measured particle size obtained using TEM and XRD data were consistent and in the 8-14 nm range. The photocatalysis activity increased with an increase in doping amounts for both remazol yellow and phenol, however, phenol requires more time for degradation than remazol yellow dye.

ACKNOWLEDGEMENTS

This work was support by the Directorate of Higher Education (DIKTI) Indonesia.

CONFLICT OF INTEREST

The authors declare that there is no conflict of interests regarding the publication of this article.

REFERENCES

1. C.A. Mirkin, *Small*, **1**, 14 (2005); https://doi.org/10.1002/smll.200400092
2. A.P. Nikalje, *Med. Chem.*, **5**, 081 (2015); https://doi.org/10.4172/2161-0444.1000247
3. G. Wang, Nanotechnology: The New Features (2018).
4. C. Lauterwasser, Opportunities and Risks of Nanotechnologies, OECD: The OECD International Futures Programme, France (2008).
5. A. Khitab, S. Ahmad, M.J. Munir, S.M.S. Kazmi, T. Arshad and R.A. Khushnood, *Rev. Adv. Mater. Sci.*, 53, 90 (2018); https://doi.org/10.1515/rams-2018-0007
6. K. Nakata and A. Fujishima, *J. Photochem. Photobiol. C: Photochem. Rev.*, **13**, 169 (2012); https://doi.org/10.1016/j.jphotochemrev.2012.06.001
7. M.S. Wong, D.S. Sun and H.H. Chang, *PLoS One*, **5**, e10394 (2010); https://doi.org/10.1371/journal.pone.0010394
8. A. Fujishima, T.N. Rao and D.A. Tryk, *J. Photochem. Photobiol. C: Photochem. Rev.*, **1**, 1 (2000); https://doi.org/10.1016/S1389-5567(00)00002-2
9. K. Hashimoto, H. Irie and A. Fujishima, *Jpn. J. Appl. Phys.*, **44**, 8269 (2005); https://doi.org/10.1143/JJAP.44.8269
10. J. Huberty and H. Xu, *J. Solid State Chem.*, **181**, 508 (2008); https://doi.org/10.1016/j.jssc.2007.12.015
11. S. Sinha, N.G.T. Orozco, D.S.A. Ramirez and R. Rodriguez-Vazquez, *J. Clean Technol.*, **4**, 411 (2009).
12. N.N. Binitha, Z. Yaakob and R. Resmi, *Cent. Eur. J. Chem.*, **8**, 182 (2010); https://doi.org/10.2478/s11532-009-0112-1
13. L. Mai, C. Huang, D. Wang, Z. Zhang and Y. Wang, *J. Appl. Surf. Sci.*, **255**, 9285 (2009); https://doi.org/10.1016/j.apsusc.2009.07.027
14. X. Lei, X. Xue, H. Yang, C. Chen, X. Li, M.C. Niu, X.Y. Gao and Y.T. Yang, *J. Appl. Surf. Sci.*, **332**, 172 (2015); https://doi.org/10.1016/j.apsusc.2015.01.110
15. E. Fakhrutdinova, A. Shabalina and E. Sudareva, *Adv. Mater. Res.*, **1085** 95 (2015); https://doi.org/10.4028/www.scientific.net/AMR.1085.95
16. T. Ohno, M. Akiyoshi, T. Umebayashi, K. Asai, T. Mutsui and M. Matsumura, *J. Appl. Catal.*, **265**, 115 (2004); https://doi.org/10.1016/j.apcata.2004.01.007
17. Y. Wang, J. Li, P. Peng, T. Lu and L. Wang, *Appl. Surf. Sci.*, **254**, 5276 (2008); https://doi.org/10.1016/j.apsusc.2008.02.050
18. H.E. Swanson and E. Tatge, Standard X-Ray Diffraction Powder Patterns, U.S. Natl. Bur. Stds. Circular 539, vol. 1 , pp. 74-76 (1953).
19. S.M. Abdel-Azim, A.K. Aboul-Gheit, S.M. Ahmed, D.S. El-Desouki and M.S.A. Abdel-Mottaleb, *Int. J. Photoenergy*, **20**, 687597 (2014); https://doi.org/10.1155/2014/687597
20. W. Ziemkowska, D. Basiak, P. Kurtycz, A. Jastrzebska, A. Olszyna and A. Kunicki, *Chem. Pap.*, **68**, 1 (2014); https://doi.org/10.2478/s11696-014-0537-7
21. P. Manurung, R. Situmeang, E. Ginting and I. Pardede, *Indones. J. Chem.*, **15**, 36 (2015); https://doi.org/10.22146/ijc.21221
22. I. Djerdj and A. Tonejc, *J. Alloys Compd.*, **413**, 159 (2006); https://doi.org/10.1016/j.jallcom.2005.02.105
23. B.A. Hunter, Rietica for 95/98/NT Version 1.71, ANSTO, Sydney (1997).
24. A. Janotti, B. Jalan, S. Stemmer and C.G. Van de Walle, *Appl. Phys. Lett.*, **100**, 262104 (2012); https://doi.org/10.1063/1.4730998
25. N. Manjula, M. Pugalenthi, V.S. Nagarethinam, K. Usharani and A.R. Balu, *Mater. Sci. Pol.*, **33**, 774 (2015); https://doi.org/10.1515/msp-2015-0115
26. N. Paul and D. Mohanta, *J. Mater. Res.*, **28**, 1471 (2013); https://doi.org/10.1557/jmr.2013.122
27. E. Huseynov, A. Garibov and R. Mehdiyeva, *J. Mater. Res. Technol*, **5**, 213 (2016); https://doi.org/10.1016/j.jmrt.2015.11.001
28. D. Chatterjee, V.P. Patnam, A. Sikdar, P. Joshi, R. Misra and N.N. Rao, *J. Hazard. Mater.*, **156**, 435 (2008); https://doi.org/10.1016/j.jhazmat.2007.12.038
29. W.I. Kim, D.J. Suh, T.J. Park and I.K. Hong, *Top. Catal.*, **44**, 499 (2007); https://doi.org/10.1007/s11244-006-0097-3
30. Z. Guo, R. Ma and G. Li, *Chem. Eng. J.*, **119**, 55 (2006); https://doi.org/10.1016/j.cej.2006.01.017
31. A. Sobczynski, L. Duczmal and W. Zmudzinski, *J. Mol. Catal. Chem.*, **213**, 225 (2004); https://doi.org/10.1016/j.molcata.2003.12.006
32. E. Grabowska, J. Reszczynska and A. Zaleska, *Water Res.*, **46**, 5453 (2012); https://doi.org/10.1016/j.watres.2012.07.048